

Validation study of ^{131}I -RRL: Assessment of biodistribution, SPECT imaging and radiation dosimetry in mice

QIAN ZHAO*, PING YAN*, LEI YIN, LING LI, XUE QI CHEN, CHAO MA and RONG FU WANG

Department of Nuclear Medicine, Peking University First Hospital, West District, Beijing 100034, P.R. China

Received November 5, 2012; Accepted February 14, 2013

DOI: 10.3892/mmr.2013.1338

Abstract. Tumor angiogenesis is important in the growth and metastasis of malignant tumors. In our previous study, we demonstrated that an arginine-arginine-leucine (RRL) peptide is a tumor endothelial cell-specific binding sequence that may be used as a molecular probe for the imaging of malignant tumors *in vivo*. The aim of the present study was to further explore the characteristics of ^{131}I -RRL by biodistribution tests, and to estimate the radiation dosimetry of ^{131}I -RRL for humans using mice data. The RRL peptide was radiolabeled with ^{131}I by a chloramine-T (CH-T) method. The radiolabeling efficiency and radiochemical purity were then characterized *in vitro*. ^{131}I -RRL was injected intravenously into B16 xenograft-bearing Kunming mice. Biodistribution analysis and *in vivo* imaging were performed periodically. The radiation dosimetry in humans was calculated according to the organ distribution and the standard medical internal radiation dose (MIRD) method in mice. All data were analyzed by statistical and MIRDOSE 3.1 software. The labeling efficiency of ^{131}I -RRL reached $70.0 \pm 2.91\%$ ($n=5$), and the radiochemical purity exceeded 95% following purification. In mice bearing B16 xenografts, ^{131}I -RRL rapidly cleared from the blood and predominantly accumulated in the kidneys, the stomach and the tumor tissue. The specific uptake of ^{131}I -RRL in the tumor increased over time and was significantly higher than that of the other organs, 24-72 h following injection ($P<0.05$). The ratio of tumor-to-skeletal muscle (T/SM) tissue exceeded 4.75, and the ratio of the tumor-to-blood (T/B) tissue peaked at 3.36. In the single-photon emission computed tomography (SPECT) imaging of Kunming mice bearing B16 xenografts, the tumors were clearly identifiable at 6 h, and significant uptake was evident 24-72 h following

administration of ^{131}I -RRL. The effective dose for the adult male dosimetric model was estimated to be 0.0293 mSv/MBq. Higher absorbed doses were estimated for the stomach (0.102 mGy/MBq), the small intestines (0.0699 mGy/MBq), the kidneys (0.0611 mGy/MBq) and the liver (0.055 mGy/MBq). These results highlight the potential of ^{131}I -RRL as a ligand for the SPECT imaging of tumors. Administration of ^{131}I -RRL led to a reasonable radiation dose burden and was safe for human use.

Introduction

Cancer is the leading cause of mortality in economically developed countries, and the second leading cause of mortality in developing countries (1). The global burden of cancer continues to significantly increase due to the aging and growth of the global population, and increasing adoption of cancer-causing behaviors, particularly smoking, within economically developing countries (2). Early diagnosis of cancer is key; however, the majority of malignancies are diagnosed and treated at the advanced stages, which leads to poor overall survival. Researchers and clinicians have increased their focus towards the specific molecular markers targeting tumorigenesis and metastasis.

It is well established that solid tumor growth is correlated with angiogenesis (3). The formation of new blood vessels, which supply metabolites to aid the survival and metastasis of tumor cells, is achieved through angiogenesis, a multi-step process that relies on the tumor-driven production of proangiogenic factors. In contrast to normal blood vessels, tumor vasculature exhibits an abnormal, incomplete endothelial lining that is characterized by large inter-endothelial junctions and an increased number of fenestrations (4).

In our previous study (5), we modified the structure of arginine-arginine-leucine (RRL) to tyrosine-RRL (tRRL; Tyr-Cys-Gly-Gly-Arg-Arg-Leu-Gly-Gly-Cys), and successfully radioiodinated it by the chloramine-T (CH-T) method. Simple biodistribution and single-photon emission computed tomography (SPECT) imaging results indicated that ^{131}I -tRRL was specifically concentrated in the tumor tissue in human PC3 prostate tumor-bearing xenografts (5). Additionally, by further experiments, Lu *et al* confirmed the cytotoxicity of ^{131}I -tRRL and revealed that tRRL adhered to tumor cells adjacent to tumor-derived endothelial cells, by an *in vitro* binding experiment and cellular uptake tests (6).

Correspondence to: Dr Rong Fu Wang, Department of Nuclear Medicine, Peking University First Hospital, 8 Xinsihou Street, West District, Beijing 100034, P.R. China
E-mail: rongfu_wang2003@yahoo.com.cn

*Co-first author

Key words: ^{131}I , peptide, tumor angiogenesis, molecular imaging, biodistribution, radiation dosimetry

In the present study, we further explored the characteristics of ¹³¹I-tRRL and estimated the radiation dosimetry of ¹³¹I-RRL for humans using mice data.

Materials and methods

Synthesis of the peptide. The sequence of tRRL (Tyr-Cys-Gly-Gly-Arg-Arg-Leu-Gly-Gly-Cys-NH₂) was designed and synthesized as described in a previous study (7). The cysteine at the C-terminal of the tRRL peptide was amidated to protect the peptide from the biocatalysts.

Radiosynthesis. Radioiodination of tRRL was performed using the CH-T method (8). The tRRL (50 μg) was dissolved in 0.5 M phosphate buffer (81 μl, pH 7.4), and ¹³¹I⁻Na (10 μl, 74 MBq) was added. Subsequently, fresh CH-T (9 μl, 10 μg/μl) was added to the mixture. The mixture was gently agitated for 1 min at room temperature, then quenched by the addition of sodium metabisulfite (45 μl, 1 μg/μl).

For routine quality control of labeling, the labeling efficiency and radiochemical purity of radiolabeled tRRL probes were calculated by paper chromatography on Xinhua filter paper (Hangzhou Xinhua Paper Industry Co., Ltd, China) with acetone and water as the mobile phase.

B16 cell culture. B16 mouse melanoma cell lines were a gift from the Department of Pathology, Peking University First Hospital (Beijing, China), and were maintained in the media recommended by the department. B16 cells were grown in RPMI-1640 medium supplemented with 10% fetal bovine serum (FBS) and 100 mg/ml penicillin-streptomycin (Gibco, Carlsbad, CA, USA). Cells were cultivated under the standard conditions of a temperature of 37°C and a humidified atmosphere of 5% CO₂. Cells were experimented with and harvested by trypsin treatment (0.25% trypsin/0.02% ethylenediaminetetraacetic acid; 3 min, 37°C) between passages 4 and 12. The cell growth status was monitored by inverted microscopy with a phase contrast microscope (CKX31 inverted microscope, Olympus, Tokyo, Japan).

Biodistribution. Animal experiments were approved by the Peking University Animal Studies Committee, according to the Guidelines for the Care and Use of Research Animals (Peking University, Beijing, China; approval ID, J201138). Forty male Kunming mice (weight, 20±3 g; age, 4-6 weeks) obtained from the Department of Laboratory Animal Science, Peking University First Hospital were used in this study. The mice were inoculated with 1×10⁷ B16 cells in the right upper limbs, and the tumors were allowed to grow to a diameter of 0.8-1.0 cm. The mice were maintained using a standard diet, bedding and environment, with free access to food and drinking water. The mice received 400 mg sodium perchlorate over 3 days for thyroid blockage.

The 40 Kunming mice were randomly divided into 8 groups of 5 mice each. The purified and isolated ¹³¹I-tRRL was diluted with 0.5 M phosphate buffer (100 μl, pH 7.4). ¹³¹I-tRRL was then injected into each mouse via the lateral tail vein. All injections were tolerated well. The animals were sacrificed by cervical dislocation at 15 and 30 min, and 1, 3, 6, 24, 48 and 72 h, following injection of the radiolabeled derivatives.

Subsequently, the mice were dissected and the tissues of interest (the blood, heart, liver, spleen, lungs, kidneys, stomach, small intestine, bladder, bone, skeletal muscle and tumor tissue) were weighed, and their radioactivities were measured using a γ-well counter along with a standard of the injection. Radioactivity results were recorded as the percentage of injected radioactivity per gram of tissue (%ID/g) corrected for background and decay.

¹³¹I-tRRL SPECT imaging in the B16 xenograft model. Four Kunming mice with B16 xenografts were used in the SPECT imaging protocol. Whole-body imaging was performed at 1, 3, 6, 24, 48 and 72 h following injection of ¹³¹I-tRRL at the Department of Nuclear Medicine, Peking University First Hospital, using SPECT imaging (SPR SPECT; GE Healthcare, Inc., Milwaukee, WI, USA) equipped with a high-energy general purpose collimator (HEGP). Whole body static images (200,000 counts) were obtained with a zoom factor of 2.0, and were digitally stored in a 256x256 matrix.

Radiation-absorbed dose calculations. The calculated mean percentages of injected activity per gram (%ID/g) for the mice organs were extrapolated to uptake in the organs of a 70-kg adult, using the standard medical internal radiation dose (MIRD) scheme along with the following formula (9,10):

$$[A_i(t)/A_0]_{human} = [A_i(t)/A_0]_{mice} \times [m_{total\ body}/m_i]_{mice} \times [m_i/m_{total\ body}]_{human}$$

where $[A_i(t)/A_0]$ is the %ID/g of source organ i administered at time t ; A_i is the radioactivity of source organ i administered at time t ; A_0 is the initial radioactivity administered at time 0; $m_{total\ body}$ is the whole body mass and m_i is the mass of source organ i .

The extrapolated values (%ID/g) in the human organs at 15 and 30 min, and 1, 3, 6, 24, 48 and 72 h, were plotted as time-activity curves (TACs). The curves were then fitted with exponential models and integrated to obtain the number of disintegrations in the source organs, using OriginPro 5.0 software (OriginLab Corporation, Northampton, MA, USA). Residence times (τ) were computed and normalized to the injected activities by calculating the area under the TACs of each organ, as follows:

$$\tau_i = \int_0^{\infty} \frac{A_i(t)}{A_0} dt$$

Where τ_i is the residence time of source organ i ; $A_i(t)$ is the radioactivity of source organ i administered at time t ; and A_0 is the initial radioactivity administered at time 0. Then, using these residence times, organ-absorbed doses and effective doses were estimated with the MIRDSE 3.1 software package (11).

Statistical analysis. All statistical analyses were performed using SPSS software (version 17.0; SPSS Inc., Chicago, IL, USA). Biodistribution data were expressed as the mean ± standard deviation, and a one-way ANOVA analysis was performed. OriginPro 5.0 and MIRDSE 3.1 software were used in the radiation dose estimations. $P < 0.05$ was considered to indicate a statistically significant difference.

Table I. Tissue biodistribution (%ID/g) of ¹³¹I-tRRL over time in mice-bearing B16 xenografts.

Tissue	15 min	30 min	1 h	3 h	6 h	24 h	48 h	72 h
Blood	6.29±0.59	4.74±0.59	4.56±0.23	2.41±0.45	1.71±0.19	0.26±0.06	0.07±0.06	0.04±0.03
Heart	2.35±0.34	1.75±0.34	1.59±0.41	0.92±0.33	1.07±0.13	0.10±0.03	0.08±0.01	0.06±0.02
Spleen	2.82±0.58	2.13±0.58	2.03±0.33	0.95±0.47	1.06±0.17	0.03±0.00	0.04±0.03	0.01±0.00
Liver	3.49±0.52	3.10±0.52	2.45±0.31	1.31±0.34	1.69±0.19	0.09±0.05	0.06±0.02	0.05±0.01
Lung	2.84±0.44	2.07±0.44	2.00±0.37	1.17±0.31	1.51±0.14	0.14±0.03	0.09±0.02	0.06±0.01
Kidney	5.29±1.31	2.86±0.41	2.65±0.32	1.61±0.09	1.35±0.30	0.09±0.01	0.06±0.02	0.04±0.00
Stomach	3.70±4.11	3.06±0.62	3.05±0.58	1.66±0.26	1.45±0.21	0.04±0.05	0.04±0.04	0.02±0.01
Small intestine	2.76±0.86	2.07±0.26	2.20±0.25	1.63±0.28	1.40±0.26	0.22±0.08	0.09±0.02	0.06±0.01
Bladder	6.17±3.00	5.38±0.44	4.87±0.52	4.82±0.55	4.45±0.18	0.41±0.09	0.40±0.08	0.35±0.11
Bone	1.47±0.12	1.25±0.12	0.91±0.27	0.73±0.22	0.78±0.14	0.10±0.02	0.09±0.02	0.04±0.02
Skeletal muscle	1.70±0.26	1.16±0.26	1.02±0.22	0.69±0.25	0.51±0.12	0.13±0.01	0.07±0.02	0.09±0.03
Tumor	3.11±0.75	2.39±0.25	2.72±0.25	2.16±0.29	2.42±0.19	0.61±0.03	0.17±0.02	0.12±0.02

Each value represents the mean 5 mice (± standard deviation) and is expressed as the percentage of injected radioactivity per gram of organ or tissue (%ID/g). tRRL, tyrosine-arginine-arginine-leucine.

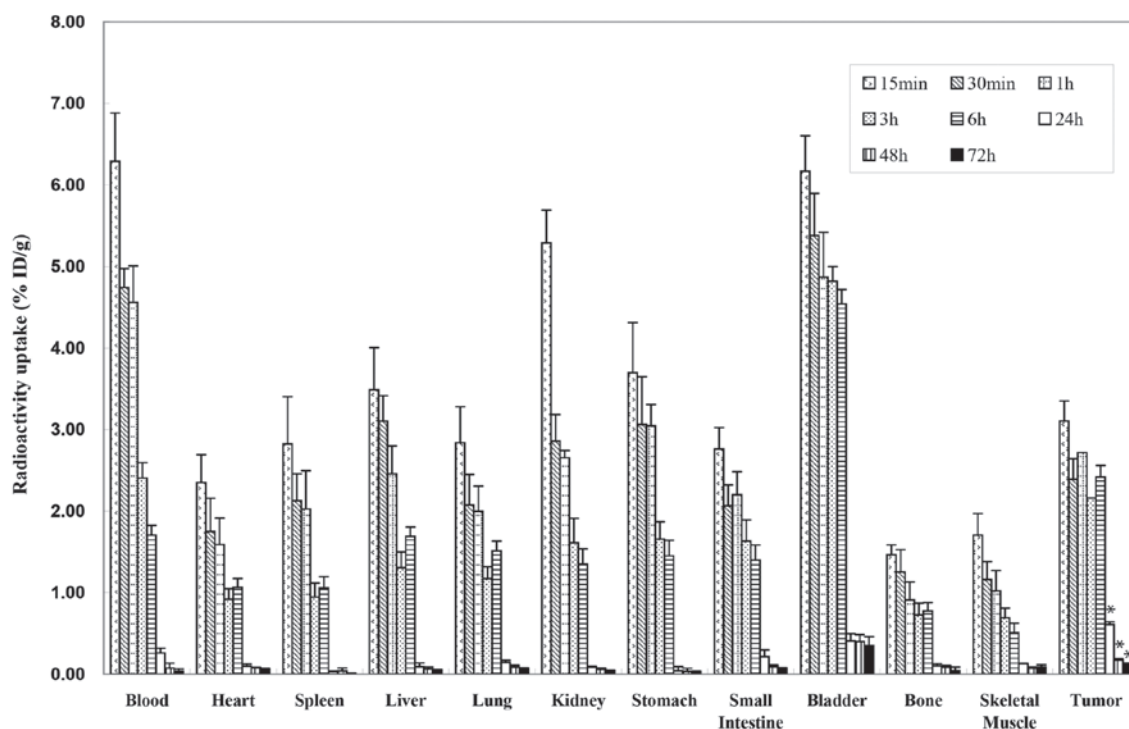


Figure 1. Biodistribution of ¹³¹I-tyrosine-arginine-arginine-leucine (tRRL) in B16 xenograft-bearing mice. The main organs and tissues, such as the heart, spleen, liver and blood, demonstrate a rapid decrease in radioactivity uptake over time. Significant radioactivity retention is evident in the tumor tissue. Data are expressed as the mean ± standard deviation (n=5), and were obtained from Table I. *P<0.05, significantly higher uptake than other organs except for bladder.

Results

Radiosynthesis. The radiolabeling efficiency of ¹³¹I-tRRL was 70±2.91% (n=5). Radiochemical purities of >95% were obtained following purification.

Biodistribution test. Biodistribution data are shown in Table I. At different time phases following injection, ¹³¹I-tRRL primarily accumulated in the kidneys and the bladder. The blood data revealed that ¹³¹I-tRRL was characterized by

rapid blood clearance, with 6.29%ID/g remaining 15 min following administration, and 2.41%ID/g remaining after 3 h. The specific uptake of ¹³¹I-tRRL in the tumor increased after 15 min, and remained at a relatively high level until 6 h following administration. Furthermore, at 24, 48 and 72 h, the tumor tissue demonstrated a higher concentration of the probe compared with the other organs (P<0.05; Fig. 1).

As a result, the ratio of tumor-to-non-tumor (T/NT) tissue accumulation following the administration of ¹³¹I-tRRL was significantly higher, particularly between 6 and 24 h. The ratio

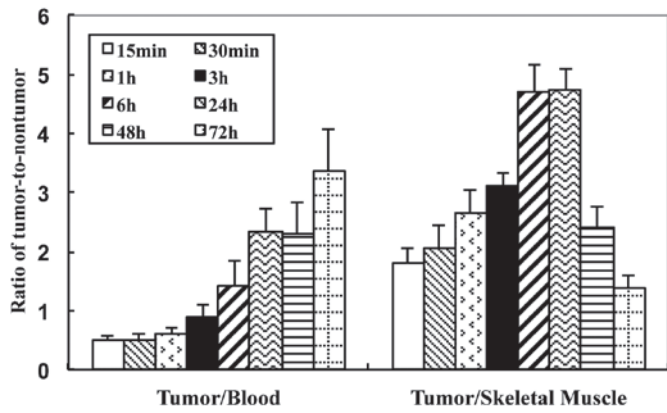


Figure 2. Tumor-to-non-tumor (T/NT) tissue ratio of blood or skeletal muscle demonstrates a better biodistribution of the probe. Ratios were calculated using the data in Table I. Data are expressed as the mean ± standard deviation (n=5).

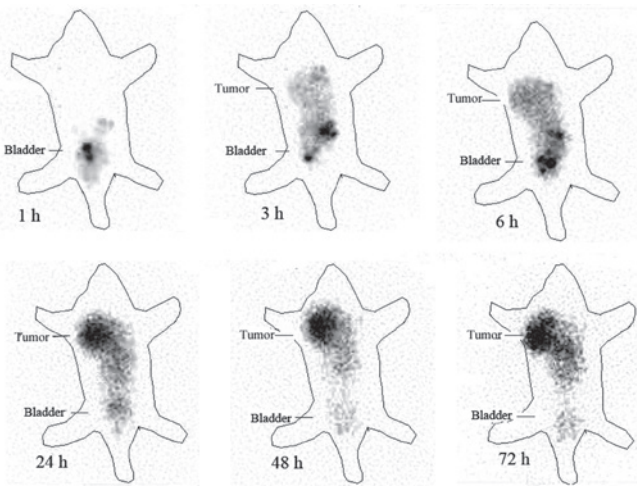


Figure 3. ¹³¹I-tyrosine-arginine-arginine-leucine (tRRL) single-photon emission computed tomography (SPECT) imaging in the B16 xenograft model. Tumors were imaged at 3 h and are clear 24 h following administration of ¹³¹I-tRRL. The tumor and bladder tissues are labeled.

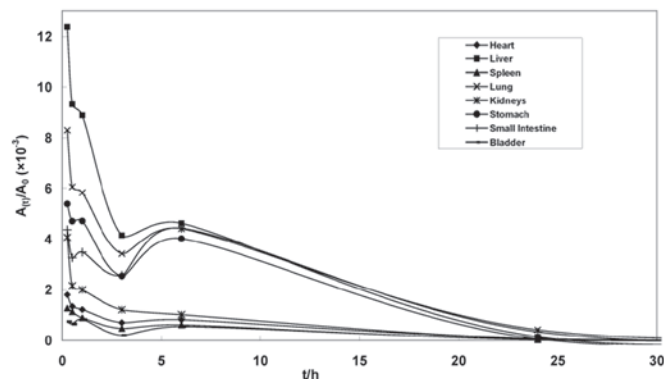


Figure 4. Typical time-activity curves (TACs) in key human organs calculated from the distribution of ¹³¹I-tyrosine-arginine-arginine-leucine (tRRL) in mice.

of tumor-to-skeletal muscle (T/SM) tissue exceeded 4.75 at the 24-h time point, and the ratio of tumor-to-blood (T/B) tissue peaked at 3.36 at 72 h (Fig. 2).

Table II. Absorbed dose of ¹³¹I-tRRL for a reference adult estimated using the mouse data.

Organ/tissue	Estimated dose (mGy/MBq) ^a
Adrenal glands	6.80E-03
Brain	9.03E-05
Breasts	2.44E-03
Gallbladder wall	8.97E-03
LLI wall	3.93E-03
Small intestine	6.99E-02
Stomach wall	1.02E-01
ULI wall	9.14E-03
Heart wall	4.64E-02
Kidneys	6.11E-02
Liver	5.55E-02
Lungs	3.81E-02
Muscle	2.34E-03
Ovaries	5.39E-03
Pancreas	1.03E-02
Red marrow	2.92E-03
Osteogenic cells	2.03E-03
Skin	1.00E-03
Spleen	4.48E-02
Testes	5.91E-04
Thymus	2.94E-03
Thyroid	6.62E-04
Urinary bladder wall	3.27E-02
Uterus	5.48E-03
Total body	5.70E-03
Effective dose	2.93E-02 mSv/MBq

^aRadiation-absorbed dose projections in humans were determined from residence times for ¹³¹I-tRRL in Kunming mice and were calculated by the use of MIRDOSE 3.1 software. Data are expressed as the mean value. tRRL, tyrosine-arginine-arginine-leucine; LLI, lower large intestine; ULI, upper large intestine.

¹³¹I-tRRL SPECT imaging in the B16 xenograft model. In mice-bearing B16 xenografts, the tumors were imaged 3 h following the administration of ¹³¹I-tRRL. Uptake of the ¹³¹I-tRRL molecular probe gradually increased over time, and a significant increase (P<0.05) in the uptake in the tumor tissues, calculated using the ROI (region of interest) technique, appeared from 24 h following intravenous injection (Fig. 3). As a result of thyroid blockage, uptake in the thyroid glands was not evident at any time point. As predicted from the biodistribution studies, the renal route of elimination of the probes also led to substantial radioactivity accumulation in the abdomen.

Radiation-absorbed dose calculations. The extrapolated values (%) in the human organs at different time points were plotted as TACs (Fig. 4).

The radiation-absorbed doses were estimated using the MIRDOSE 3.1 software and the mean values obtained are shown in Table II, which lists the individual organ

radiation-absorbed doses and the individual effective dose (ED) results of the estimated radiation doses for humans as mGy/MBq and mSv/MBq administered with ^{131}I -tRRL, with the data derived from the mouse data. The ED for the adult male dosimetric model was estimated to be 0.0293 mSv/MBq. Higher absorbed doses were estimated for the stomach (0.102 mGy/MBq), the small intestines (0.0699 mGy/MBq), the kidneys (0.061 mGy/MBq) and the liver (0.055 mGy/MBq). The unit density sphere model was applied to a 2-g tumor, and the estimated absorbed dose was 0.015 mGy/MBq.

Discussion

Tumor angiogenesis is important in the growth and metastasis of malignant tumors. An increasing number of studies are focusing on radiolabeled molecular probes, which target newly formed tumor vessels (12-16).

Our previous *in vivo* study in nude mice demonstrated that ^{131}I -tRRL had potential for mapping tumor angiogenesis (5). Radiolabeled molecules are important in evaluating tumor characteristics, such as aggressiveness and angiogenesis, and in identifying the effectiveness of cancer treatments, such as chemotherapy and radiotherapy (17).

The tripeptide sequence RRL was previously considered to be a tumor endothelial cell-specific binding sequence by an *in vitro* bacterial peptide display library panned against tumor cells derived from SCC-VII murine squamous cell carcinomas. The fluorescent RRL studies demonstrated that the peptide preferentially adhered to the tumor vasculature *in vivo*, and the target was not only tumor-specific but also endothelial in location (18).

In our previous study, we modified the structure of RRL by adding tyrosine to its amino terminal, and termed this tRRL. We then radiolabeled the tRRL with ^{131}I using the CH-T method. The biodistribution data of ^{131}I -tRRL and the *in vivo* imaging demonstrated prospective application in BALB/c nude mice-bearing PC3 human prostate carcinoma xenografts (5). Further study confirmed the non-cytotoxicity of tRRL, although ^{131}I -RRL caused significant cytotoxicity in HepG2 cells. An *in vitro* binding experiment using fluorescein isothiocyanate (FITC) demonstrated improved adherence between tRRL and different types of tumor cells (6). Lu *et al* also hypothesized that VEGFR-2 is not the sole binding ligand for tRRL targeting tumor angiogenic endothelium, and that radioiodinated tRRL may be a non-invasive method for functional molecular imaging of tumor angiogenesis (19).

In the present study, we further explored the characteristics of ^{131}I -tRRL and the safety of the new radiotracer. The radiolabeling efficiency and radiochemical purities of ^{131}I -tRRL were similar to what had been previously found (5). Within 1 h following administration of the molecular probe, the probe mainly accumulated in the blood, the kidneys and the bladder. We considered the higher concentration in the kidneys and the bladder to reflect the excretion pathway of ^{131}I -tRRL. The blood data revealed that ^{131}I -tRRL was characterized by rapid blood clearance, with 6.29%ID/g remaining 15 min following administration and 2.41%ID/g remaining after 3 h (i.e., >60% of the probe was metabolized to other organs and tissues). The specific uptake of ^{131}I -tRRL in the tumor tissue increased after 15 min and remained at a relatively high level until

6 h following administration. Furthermore, from 24 to 72 h following administration of the probe, a higher accumulation of the probe was observed in the tumor tissue compared with the other organs ($P < 0.05$), except for the bladder. The higher ratio of T/NT tissue is also a marker for evaluating a potential oncologic radiotracer. The ratio of T/B and T/SM tissue revealed a good ratio of T/NT tissue (Fig. 2). The highest T/B tissue ratio was 3.36 (at 72 h), and the highest T/SM tissue ratio was 4.76 (at 24 h), following injection of ^{131}I -tRRL.

Arginine-glycine-aspartate (RGD) peptide is a widely studied angiogenesis-specific targeting peptide. The rapid blood clearance and high tumor uptake of ^{131}I -tRRL was similar to the results on cyclic RGD radiolabeled with $^{99\text{m}}\text{Tc}$, which is integrin $\alpha_v\beta_3$ -specific and widely used in integrin expression imaging. Zhang *et al* studied the radiosynthesis and biodistribution of the ^{131}I -RGD dimer in melanoma xenografts. The results demonstrated that the ratios of T/SM and T/B were 4.42 and 2.27 at 24 h, respectively, which were similar to the results of the present study (20).

The results of the SPECT imaging using ^{131}I -tRRL paralleled the biodistribution results. *In vivo* scintigraphic imaging revealed a higher tumor uptake in the mice-bearing B16 xenografts. From the biodistribution data and the SPECT images, the most suitable acquisition time for tumor imaging is 24 h following administration of ^{131}I -tRRL. The images were clearer than Yu *et al* and Lu *et al* reported (5,19).

Continual imaging of the xenografts of mice-bearing B16 xenografts revealed that ^{131}I -tRRL accumulated in the organs of the renal system, the stomach and the small intestine, which partially contributed to its clearance from the circulatory system. This partly explains the reason for the higher radiation doses estimated for the stomach, small intestine and liver.

The safety of a radioligand is determined by its toxicity and radiation. Lu *et al* confirmed the non-cytotoxicity of tRRL by *in vitro* experiments. The present study evaluated the absorbed radiation dose of ^{131}I -tRRL in humans (6).

In nuclear medicine, the most commonly used method for the calculation of internal radionuclide dose estimates was developed by the MIRD Committee and most recently summarized in the MIRD Primer (21). The mouse biodistribution data was translated into patient dose estimations, and the organ values were extrapolated from this to a 70 kg adult using the standard MIRD scheme and S tables.

The ED for the adult male dosimetric model was estimated to be 0.0293 mSv/MBq, which is lower than that of ^{131}I -MIP-1145 used in the treatment of stage III and IV melanoma (22). Higher absorbed doses were estimated for the stomach (0.102 mGy/MBq), the small intestines (0.0699 mGy/MBq), the kidneys (0.0611 mGy/MBq) and the liver (0.055 mGy/MBq). Beer *et al* studied the dosimetry of an RGD probe (^{18}F -Galacto-RGD) clinically studied in humans (23). It was found that the effective radiation dose of the ^{18}F -labeled RGD tracer was similar to that of ^{18}F -FDG, and that the tracer could be safely and effectively used for imaging integrin $\alpha_v\beta_3$ in humans. The effective dose of ^{131}I -tRRL (2.93 mGy/MBq) was higher than that of ^{18}F -Galacto-RGD (18.7 $\mu\text{Gy/MBq}$). The different dosimetry was most likely to be due to the different isotopic characteristics.

In conclusion, current radiation dosimetry estimates for ^{131}I -tRRL from non-human primates have demonstrated the

safety of ¹³¹I-tRRL and its potential for use in humans. The results of the present study highlight the potential of ¹³¹I-tRRL as a ligand for the SPECT imaging of tumor angiogenesis. Administration of ¹³¹I-tRRL led to a reasonable radiation dose burden and was safe for human use.

Acknowledgements

This study was supported by grants from the Natural Science Foundation of China (NSFC; grant nos. 30870729 and 81071183); the Ministry of Science and Technology of China (Projects 2011YQ030114 and 2011YQ03011409); the Research Fund for the Medicine and Engineering of Peking University (Beijing, China; Fund BMU20120297); the Research Fund of the Key Laboratory of Radiopharmaceuticals, Beijing Normal University, China; the Ministry of Education, Department of Chemistry, Beijing Normal University (110202 and 120201). The authors would like to thank Yan Rong Du and Chunli Zhang for their help in using the MIRDOSE 3.1 software, and acknowledge the contributions of the research group of the Department of Nuclear Medicine, Peking University First Hospital (Beijing, China).

References

1. The Global Burden of Disease: 2004 update. World Health Organization, Geneva, pp2-26, 2008.
2. Jemal A, Bray F, Center MM, Ferlay J, Ward E and Forman D: Global cancer statistics. *CA Cancer J Clin* 61: 69-90, 2011.
3. Glunde K, Pathak AP and Bhujwalla ZM: Molecular-functional imaging of cancer: to image and imagine. *Trends Mol Med* 13: 287-297, 2007.
4. Fukumura D and Jain RK: Tumor microvasculature and micro-environment: targets for anti-angiogenesis and normalization. *Microvasc Res* 74: 72-84, 2007.
5. Yu M, Zhou H, Liu X, Huo Y, Zhu Y and Chen Y: Study on biodistribution and imaging of radioiodinated arginine-arginine-leucine peptide in nude mice bearing human prostate carcinoma. *Ann Nucl Med* 24: 13-19, 2010.
6. Lu X, Yan P, Wang R, Liu M, Yu M, Zhang C and Guo F: The further study on radioiodinated peptide Arg-Arg-Leu targeted to neovascularization as well as tumor cells in molecular tumor imaging. *J Radioanal Nucl Ch* 290: 623-630, 2011.
7. Yu MM, Wang RF, Yan P, Zhang CL, Liu M and Cui YG: Design, synthesis and iodination of an Arg-Arg-Leu peptide for potential use as an imaging agent for human prostate carcinoma. *J Label Compd Radiopharm* 51: 374-378, 2008.
8. Matloobi M, Rafii H, Beigi D, Khalaj A and Kamali-Dehghan M: Synthesis of radioiodinated labeled peptides. *J Radioanal Nucl Ch* 257: 71-73, 2003.
9. Stabin MG and Siegel JA: Physical models and dose factors for use in internal dose assessment. *Health Phys* 85: 294-310, 2003.
10. Molina-Trinidad EM, de Murphy CA, Ferro-Flores G, Murphy-Stack E and Jung-Cook H: Radiopharmacokinetic and dosimetric parameters of ¹⁸⁸Re-lanreotide in athymic mice with induced human cancer tumors. *Int J Pharm* 310: 125-130, 2006.
11. Stabin MG: MIRDOSE: personal computer software for internal dose assessment in nuclear medicine. *J Nucl Med* 37: 538-546, 1996.
12. Kim YH, Jeon J, Hong SH, *et al*: Tumor targeting and imaging using cyclic RGD-PEGylated gold nanoparticle probes with directly conjugated iodine-125. *Small* 7: 2052-2060.
13. Engle JW, Hong H, Zhang Y, *et al*: Positron emission tomography imaging of tumor angiogenesis with a ⁶⁶Ga-labeled monoclonal antibody. *Mol Pharm* 9: 1441-1448.
14. Zhou Y, Chakraborty S and Liu S: Radiolabeled cyclic RGD peptides as radiotracers for imaging tumors and thrombosis by SPECT. *Theranostics* 1: 58-82, 2011.
15. Edwards WB, Akers WJ, Ye Y, *et al*: Multimodal imaging of integrin receptor-positive tumors by bioluminescence, fluorescence, gamma scintigraphy, and single-photon emission computed tomography using a cyclic RGD peptide labeled with a near-infrared fluorescent dye and a radionuclide. *Mol Imaging* 8: 101-110, 2009.
16. Liu S, Liu H, Jiang H, Xu Y, Zhang H and Cheng Z: One-step radiosynthesis of ¹⁸F-AIF-NOTA-RGD₂ for tumor angiogenesis PET imaging. *Eur J Nucl Med Mol Imaging* 38: 1732-1741.
17. Tabar EB, Lambrecht FY, Gunduz C and Yucebas M: *In vitro* evaluation of apoptosis detection by ^{99m}Tc-tetrofosmin in MCF-7 breast cancer cell line. *J Radioanal Nucl Ch* 288: 839-844, 2011.
18. Weller GE, Wong MK, Modzelewski RA, *et al*: Ultrasonic imaging of tumor angiogenesis using contrast microbubbles targeted via the tumor-binding peptide arginine-arginine-leucine. *Cancer Res* 65: 533-539, 2005.
19. Lu X, Yan P, Wang RF, Liu M, Yu MM and Zhang CL: Use of radioiodinated peptide Arg-Arg-Leu targeted to neovascularization as well as tumor cells in molecular tumor imaging. *Chinese J Cancer Res* 24: 52-59, 2012.
20. Zhang CL, Wang RF, Zhang L, *et al*: (¹³¹I) labeling and bioactivity evaluation of a novel RGD dimer targeted to integrin $\alpha\beta_3$ receptor. *J Peking Univ Health Sci* 43: 295-300, 2011 (In Chinese).
21. Loevinger R, Budinger TF and Watson E (eds): *MIRD primer for absorbed dose calculations*. Society of Nuclear Medicine, New York, pp1-21, 1988.
22. Joyal JL, Barrett JA, Marquis JC, *et al*: Preclinical evaluation of an ¹³¹I-labeled benzamide for targeted radiotherapy of metastatic melanoma. *Cancer Res* 70: 4045-4053, 2010.
23. Beer AJ, Haubner R, Wolf I, *et al*: PET-based human dosimetry of ¹⁸F-galacto-RGD, a new radiotracer for imaging alpha v beta3 expression. *J Nucl Med* 47: 763-769, 2006.